Supplementary Information for

Microscopic charcoals in ocean sediments off Africa track past fire intensity from the continent

Aritina Haliuc[1*+], Anne-Laure Daniau[1*], Florent Mouillot[2], Wentao Chen[2], Bérangère Leys[3], Valérie David[1], Vincent Hanquiez[1], Bernard Dennielou[4], Enno Schefuß[5], Germain Bayon[4], Xavier Crosta[1]

[1]Univ. Bordeaux, CNRS, Bordeaux INP, EPOC, UMR 5805, F-33600 Pessac, France

[2]UMR CEFE, Univ. Montpellier, CNRS, EPHE, IRD, Univ. Paul Valery Montpellier 3, 1919 route de Mende, 34293, Montpellier, CEDEX 5, France

[3]Aix Marseille Univ, Avignon Univ, CNRS, IRD, IMBE, Aix Technopole de l'environnement Arbois Méditerranée Avenue Louis Philibert - Batiment Villemin 13545 Aix-en-Provence Cedex 4, France

[4]Univ Brest, CNRS, Ifremer, Geo-Ocean, F-29280 Plouzané, France

[5]MARUM – Center for Marine Environmental Sciences, University of Bremen, Leobener Strasse 8, 28359 Bremen, Germany

Email: aritinahaliuc@gmail.com

anne-laure.daniau@u-bordeaux.fr

[+]Present address: Stefan cel Mare University of Suceava, MANSiD, Universitatii 13, 720229 Suceava, Romania; Romanian Academy, Institute of Speleology, 5 Clinicilor, Cluj-Napoca, 400006, Romania

1. Microcharcoal pathways from land to ocean floor

At the production site (Supplementary Figure 1 A), vegetation burning produces and releases charcoal particles and other particulates (gases, ash) of different sizes which are transported to the sink (ocean floor) (Supplementary Figure 1 B). A fraction of the charcoal particles is dispersed into the air and,

depending on the meteorological conditions (Viegas, 1997; Garstang et al., 1997; Palmer, Northcutt, 1975; Garstang et al., 1997) is carried aloft long distance (1), another fraction is immediately falling out (aerial fall-out) in the vicinity of the combustion site while another fraction remains on the ground and is washed away by runoff process entering the river system (Supplementary Figure 1) (Patterson et al., 1987, Clark, 1988, Radke et al., 1991; Viegas, 1997; Peters, Higuera, 2007; Vachula, Richter, 2017).

The sedimentary charcoal record is influenced by the characteristics at the production source (fuel type, amount, fire size, intensity and severity (Chrzazvez et al., 2014; Umbanhowar and McGrath, 1998; Mastrolonardo et al., 2017) which dictate the quantity of charcoal produced. In addition, the charcoal record is also influenced by aerial (Supplementary Figure 1, 1), waterborne – fluvial and marine (Supplementary Figure 1, 2) transport which determine the distance where charcoal is carried and also by sedimentation (settling, bioturbation, fossilization and accumulation) processes (Clark et al., 1998 a, b; Zhao et al. 2016; Patterson et al., 1987).

Some particles with low critical velocity or those found at the edges of the plume, where the force of the convection currents is low, are lost and fall (back) on the surface (Patterson et al., 1987, Clark, 1988). The scale-dependent atmospheric circulation, e.g., the horizontal and vertical currents but also wind speed and direction, is important for aerial transport (Patterson et al., 1987; Garstang et al., 1997). Experimental fires show that crown fires generate stronger convection columns than surface fires which can lift the particles more than 5 km in the air (Clark et al., 1998; Stocks and Kauffman, 1997; Garstang et al., 1997). A distance-decay rule from the source to the sink might be expected (Clark, 1988; Clark and Royal, 1996, 1995; Patterson et al., 1987). The distance travelled by charcoal is debated and ranges from tens of meters (Clark et al., 1998; Lynch et al., 2004) to tens or more of kilometres (Peters and Higuera, 2007; Vachula, 2018; Vachula and Richter, 2018; Adolf et al., 2018; Duffin et al., 2008; Leys et al., 2015 (Supplementary Figure 1, 1). These particles can sink (Supplementary Figure 1, 4) from the atmosphere

on the ocean surface and/or can be washed out by the rain (Supplementary Figure 1, 3). Rolling and saltation can occur on the riverbed and move the particles alongside (Nichols et al., 2000).

Studies based on marine sediment traps show that organic and lithogenic particles reach the sea floor in 10 days to 1 month with a sink velocity of ~100 m/day (Hooghiemstra et al., 2006; Dupont, 1999) while laboratory experiments show that once in the water, charcoal initially floats but becomes completely waterlogged and sinks in a matter of hours given their porosity (Davis et al., 1967, Nichols et al., 2000). The particle settling within the ocean water column is relatively quick. On a continental scale the ocean currents influence on particle settling is relatively low, however, on local scale, the settling is influenced by the oceanic conditions (currents) and the horizontal mixing (Supplementary Figure 1, 5, 6, 7) (Hooghiemstra et al., 2006). In the ocean, charcoal might get attached on the surface of other particles like faecal pellets (produced by marine organisms) and filamental aggregates or enter the marine food chain and sink gravitationally to the ocean floor similarly to pollen (Hooghiemstra et al., 2006; Dupont, 1999). The influence of ocean currents on the pollen distribution in marine sediments is low and we anticipate the same impact on microcharcoal distribution in our marine samples (Dupont, Wyputta, 2003).

In deep-sea sediments far from the coast and off arid regions where the hydrographic system is missing but the atmospheric wind system is strong, like NW Africa, the aeolian transport is the dominant carrier of fine particles (Dupont et al., 2011). In this case, it is expected that aeolian charcoal is much rapidly/sooner transported and deposited than waterborne charcoal (Patterson et al., 1987).

The microcharcoal particles settling on the ground and/or directly on the surface of the lakes and river in the vicinity of combustion source are removed by surface flow (runoff, rivers) and enter the fluvial system which carry them as suspended load to the sink, herein the ocean (Clark and Patterson, 1997) (Supplementary Figure 1, 2). Nonetheless, fluvial transport is more important in humid tropical regions, such as W Africa, where the rainfall intensity and frequency is high enough to assure a well-developed

hydrographic system and runoff activity and/or in areas where soil infiltration is low and the hydrographic basin has steep slopes (Clark, 1988; Dupont, 1999; Patterson et al., 1987).

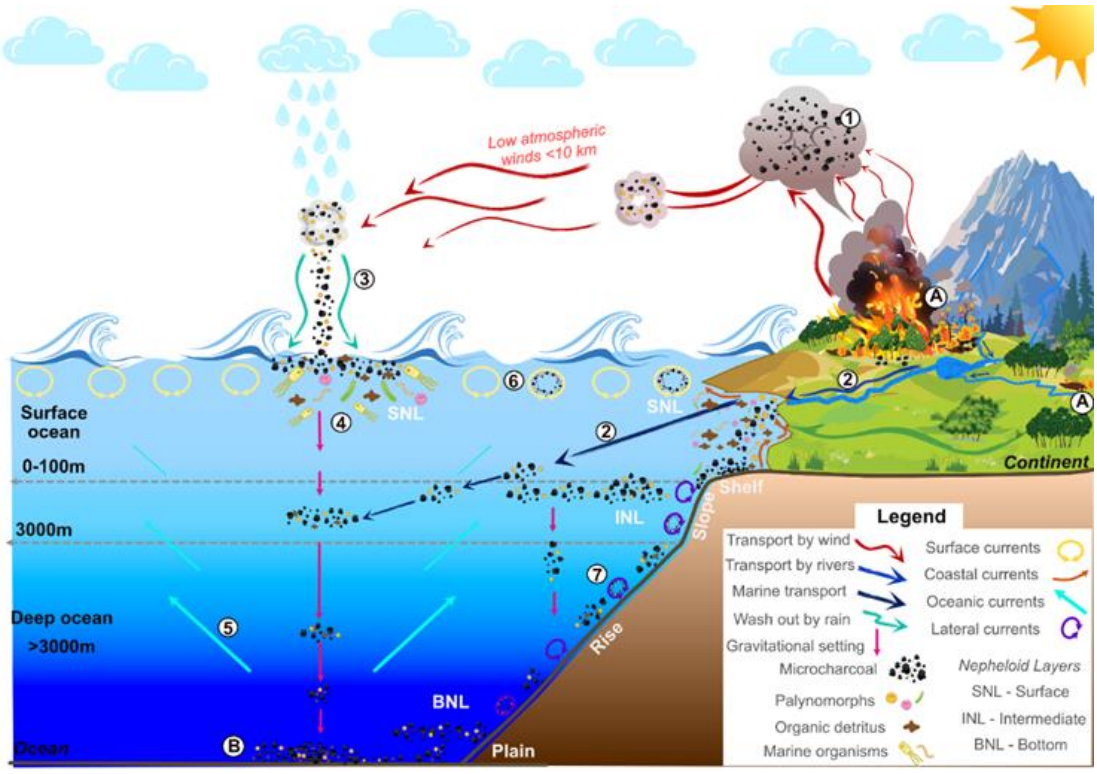

Supplementary Figure 1. The microcharcoal pathways from the source of combustion to the sink on the ocean floor. For number and letter explanations, please consult the text.

2. Dispersion modelling of fire plumes and charcoal particles deposition

Plume numerical modelling simulation in North America estimates that microcharcoal particles are lifted by thermal (buoyancy) convection (Vachula et al., 2018) to great heights depending on the fire radiative power (Sofiev et al., 2013). Results from different studies (e.g., Peters and Higuera, 2007; Vachula, 2018; Vachula and Richter, 2018; Adolf et al., 2018; Duffin et al., 2008; Leys et al., 2015) show

that (macro/micro) charcoal travels between few hundred metres to few hundred kilometres from the fire site. Comparisons between lacustrine sedimentary records and modelling of charcoal dispersal (Peters and Higuera, 2007; Vachula, 2018; Vachula and Richter, 2018) are available only for lakes from North America. No aeolian information regarding particle transport from land to the ocean is available for Africa.

Despite the great interest in charcoal particles' atmospheric dispersal in continental settings (for example, Peters and Higuera, 2007; Vachula, 2018; Vachula and Richter, 2018), the restricted spatial settings preclude a complex overview on charcoal behaviour. Some models were run using Hysplit smoke dispersal properties (prescribed burns) (Draxler, Hess, 1998). However, prescribed burns look at a very small size, $PM_{2.5}$ emissions, which have similar physical behaviour with gases than with charcoal particles. Backward air trajectories were used to estimate the potential source area of different fire proxies such as charcoal (Osmont et al. 2020) or monosaccharide anhydrides (MA) in lake and ice core records (Dietze et al., 2020; Legrand et al., 2016; Grieman et al., 2018). Using only air trajectories, the study of Hicks and Isaksson (2006) suggested charcoal can be transported over 1500 km distances.

Osmont et al. (2020) used backward air trajectories and a global aerosol-climate model ECHAM6.3-HAM2.3 using dry and wet deposition to simulate the transport of Black Carbon and charcoal of about 5µm size. They hypothesised that microcharcoal >10µm observed in a snow pit of the Swiss Alps originated from fires in Portugal.

To estimate the potential aeolian transport of microcharcoal from the African continent to the ocean, we modelled the fire plume dispersion and deposition of charcoal particles with the Hybrid Single-Particle Lagrangian Integrated Trajectory model (Hysplit)'s plume dispersion model and computation of particle concentration. We used the default 3-dimensional particle distribution (horizontal and vertical) with dry and wet deposition in the "deposit particles not reducing their mass" mode. Hysplit's air dispersal and deposition model simulates the distribution of a gaseous or particulate-phase pollutant following

dispersive motion. This simulation uses a fixed number of particles which are advected by a wind field, spread by a turbulent component and, in our case, removed by dry and wet mechanisms (Draxler, Hess, 1998). Although, to our knowledge, Hysplit's air dispersal and deposition model was not tested yet against empirical charcoal observations, we anticipated a better identification of charcoal aerial source areas compared to using air trajectories only. The model was tested in 10 different fire locations strategically chosen to cover different environmental settings across our study zones (Fig. S.2). These test runs were intended to parametrize the simulations in order to evaluate and establish the settings which best characterise the fires in our study area and to assess the model sensitivity. We run the model at three atmospheric levels using three microcharcoal particle sizes that describe the range of our dataset.

Firstly, the model was tested in different deposition settings with no deposition, wet only, dry only and both wet-dry deposition. Different time releases for the fire plume, spanning between 1, 12, 24, 72, 96, 120, 144, 168 h, were also tested. We established the time travelled by the fire plume to 96 h, which is equivalent to how far the fire plume goes in this time interval. We run the model for different emission hours representing the time of the fire event or the time span for the fire to consume the fuel in a given location. Given that fires consume the total biomass in one location (represented by a pixel) and then move forward to another pixel, we decided to use 1h of emission so a given quantity of charcoal particles is released in this time. The time of the fire event was set in the middle of the day after testing the model at different times over the day and night. The day of the emission was settled according to the information from the FRY version 2 database, so that each fire event was chosen from the fire season specific to each location and represents a real fire. The number of particles released during the fire event was tested for different quantities spanning between 1 to 5000 particles, but we noticed there is no change in the plume dispersal and deposition after 2500 particles. In other words, even if there are more particles released during a fire event the percentage of particles deposited stays the same.

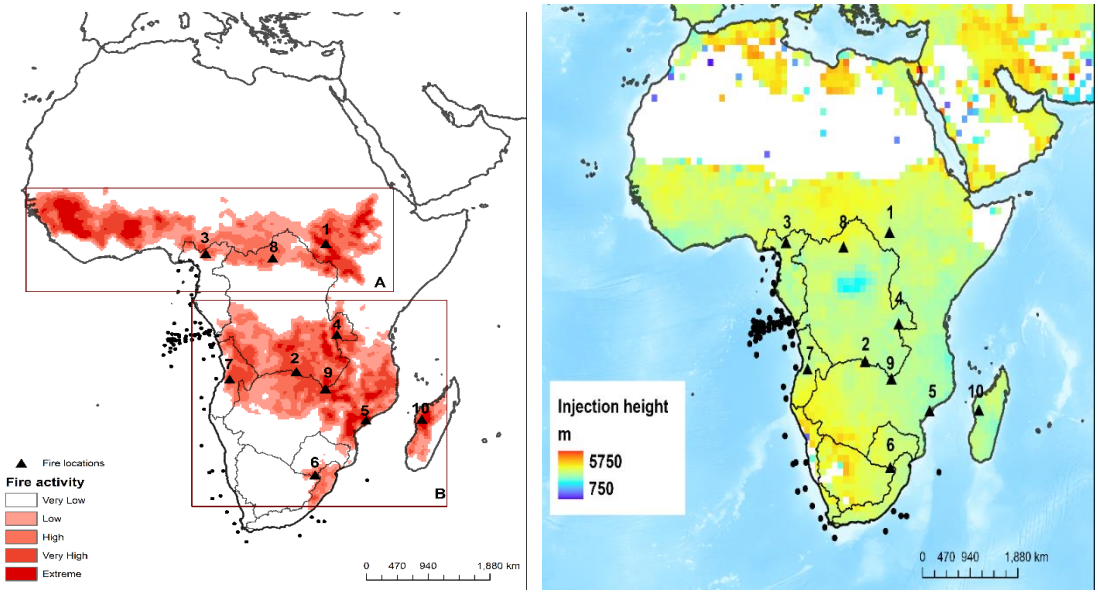

Supplementary Figure 2. Fire regions defined by fire number density (FRY version 2) and the fire location (triangle) for dispersal modelling tests (left panel). The fire injection height (99 percentile) for 2010 (Sofiev et al., 2013) (right panel)

Given the high sensitivity of the model to the defined height (m above the surface), we decided to run the models at specific heights (atmospheric level) to capture the full range of atmospheric transport and reduce the influence of the lower (close to surface) mixed atmospheric layer. The model height is equivalent with the altitude of the fire plume/injection height and was estimated from Sofiev et al. (2012). The plume concentration and deposition grid spacing was set to 0.05º x 0.05º and the span was set to 30º x 30º.

The simulations were run with three particle size diameters, 10 µm, 13 µm and 92 µm, representing the minimum, the median and the maximum of all charcoal assemblages in our database. Particle settling velocity for each size of irregularly shaped particle was estimated following Vachula, Richter (2017), as irregularly shaped particles travel a much greater distance. Particle density was set to 0.5 g/cm^3 following Vachula, Richter (2017). Particle shape was set to 1 (using Stokes equation for particle fall speed) for 10

and 13 µm particles and -1 for 92 µm particles (using Ganser equation which accounts for turbulent drag for particles bigger than 20 µm) (Dare, 2015).

For each location we estimated the charcoal concentration within the plume, the likely charcoal deposition (%) and corresponding particle deposition area (km) which represent the maximum distance travelled by the plume. We performed tests in 10 locations. For the fire test located close to the ocean, for example location 6 and 10, the model was not able to perform calculations due to the complex atmospheric circulation with an interplay between continental and oceanic air-masses. The plume and the depositional area were directly proportional with injection height if there were no major interactions between oceanic and continental air-masses and no major changes in the boundary layer and geographic conditions.

The models showed similar results independent of fire locations and particle size and for ease of interpretation we present the results from Location 1 and 2 (Fig. S.2 and S.3, Supplementary Table 1). A high proportion of particles (90-99%) are deposited close to the fire site between 15 and 45 km for low and middle atmospheric levels, regardless of their size, whereas small particles are deposited up to 160-290 km for high atmospheric levels. A small proportion (1%) of microcharcoal may travel much further away, up to 1800 km (Supplementary Table 1).

Supplementary Table 1. Table showing settings and results from Hysplit air dispersal and deposition model for two test fire locations

Plume column (altitude, m)		Hours	Particle Diameter (µm)	1			2			
Bottom	Top			Likely deposition (%)	Likely deposition (km)	Plume (max km travelled)		Likely deposition (%)	Likely deposition (km)	Plume (max km travelled)
4000	**5000**	**96**	**10**	99	160	1300		99	270	1800
			13	99	160	1300		99	290	1700
			92	90	45	230		90	25	180

1250	**2250**	**96**	**10**	99	45	1300	90	40	1500
			13	99	45	1300	90	40	1500
			92	90	45	100	90	35	120
250	**500**	**96**	**10**	90	20	400	90	25	600
			13	90	20	400	90	25	500
			92	90	15	55	90	20	50
Fire location altitude				***400m***				***1400m***	

Our estimates for all charcoal particle size for the mid and low atmospheric level, agrees with previous estimates from continental studies showing that (functional) source area for (micro- and macro-) charcoal particles fall within few dozen km (Vachula, 2018; Snitker, 2018; Peters and Higuera, 2007; Vachula and Richter, 2018; Clark, 1988). Our model adds more nuances to previous work based on air back trajectories (Hicks and Isaksson, 2006) or charcoal (5µm) (Osmont et al., 2020) simulations on charcoal source-area on land indicating that only a small fraction of the microscopic particles can travel thousands of km away from the source.

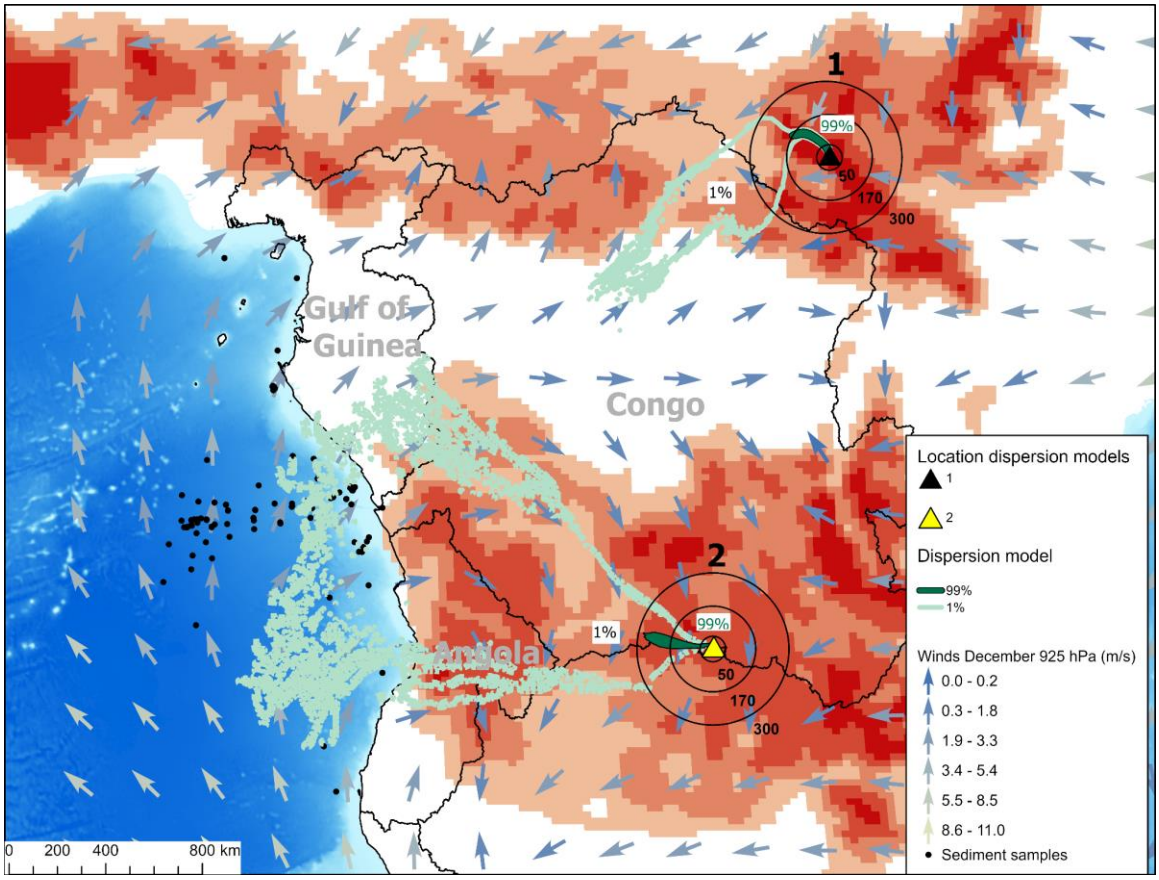

Supplementary Figure 3 The fire dispersion and deposition model at a 4000-5000 m injection height for location 1 and location 2 showing the fire plume dispersal and likely deposition (%) of microcharcoal particles. The red background represents fire activity. The map presents the case scenario with the highest injection height corresponding to the maximum distance travelled by microscopic charcoal particles.

Using this air dispersal and deposition model, we suggest that most of the microscopic charcoal stays within a few tens to a few hundreds of kilometres from the fire area. As winds transport only a small proportion of particles over longer distances, we suggest a minor mixing of charcoal between hydrographic basins. Fig. S.3 shows plume dispersion of concentration for locations 1 and 2. Location 1 is close to the Congo hydrographic basin, at the northern edge of the basin. Location 2 is located on the southern border of the Congo. Results show that most of the microscopic charcoal particles (99%) stay

very close to the fire site within hundreds of km and only a small proportion (1%) travels thousands of km away from the site. We thus suggest that the majority of charcoal transported by wind fall within the hydrographic basin limit from where they were produced, are washed and deposited in rivers and then transported by the fluvial system to the ocean. The fluvial and wind source areas overlap and there is a very small proportion of particles coming from another hydrographic basin.

Considering the closed land-sea link between pollen assemblages in marine sediments and latitudinal vegetation distribution in Africa (Dupont, 2011; Dupont et al., 2019; Dupont, Wyputta, 2003; Hooghiemstra et al., 1986; Zhao et al., 2016), we anticipate microcharcoal deposited in marine sediments come from the closest hydrographic basins and reflect spatial fire regimes distribution.

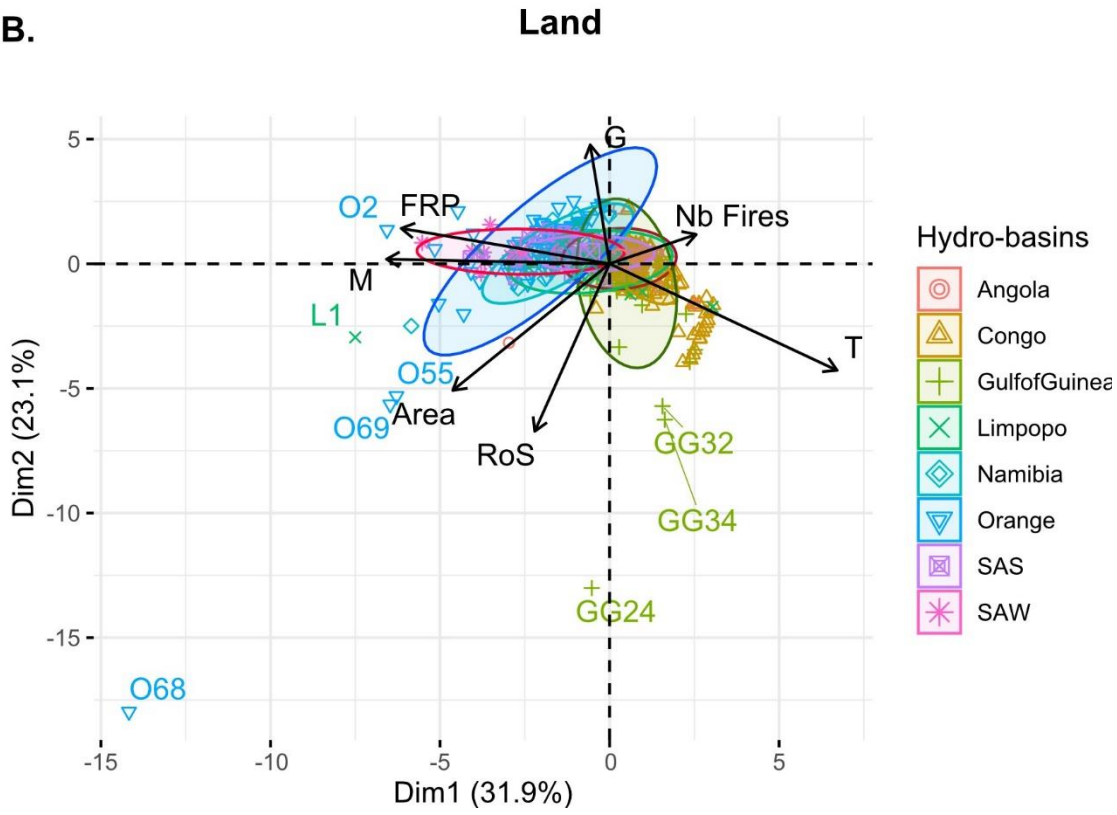

Supplementary Figure 4 Results from the principal component analysis on land fire parameters (derived from FRY2 version at 1°x1° grid) including fire number, area (ha), mean fire radiative power

(FRP, W/m^2), rate of spread (RoS) for major burnt vegetation types (G – Graminoids, M – Mixed, T - Trees). Ellipses with different colors and symbols represent the hydro-basins (please note that Namibia and Limpopo don't form an ellipse on the ocean data due to the restricted number of particles).

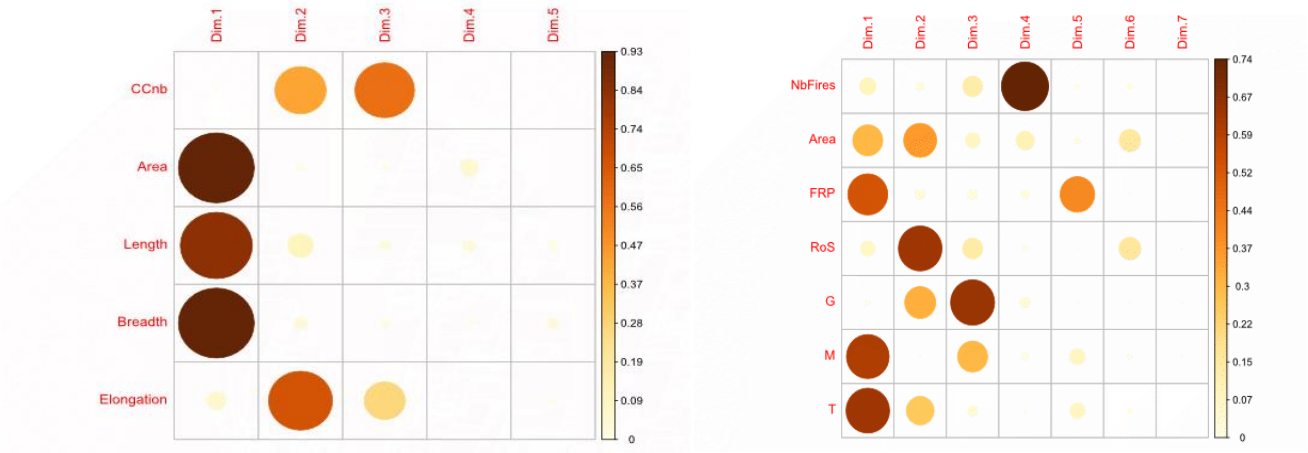

Supplementary Figure 5. Quality of representation (COS2) of ocean microcharcoal (left) and fire land (right) variables on all the dimensions. The circle represent the goodness-of-fit, cos^2 for the variables on PC dimensions.

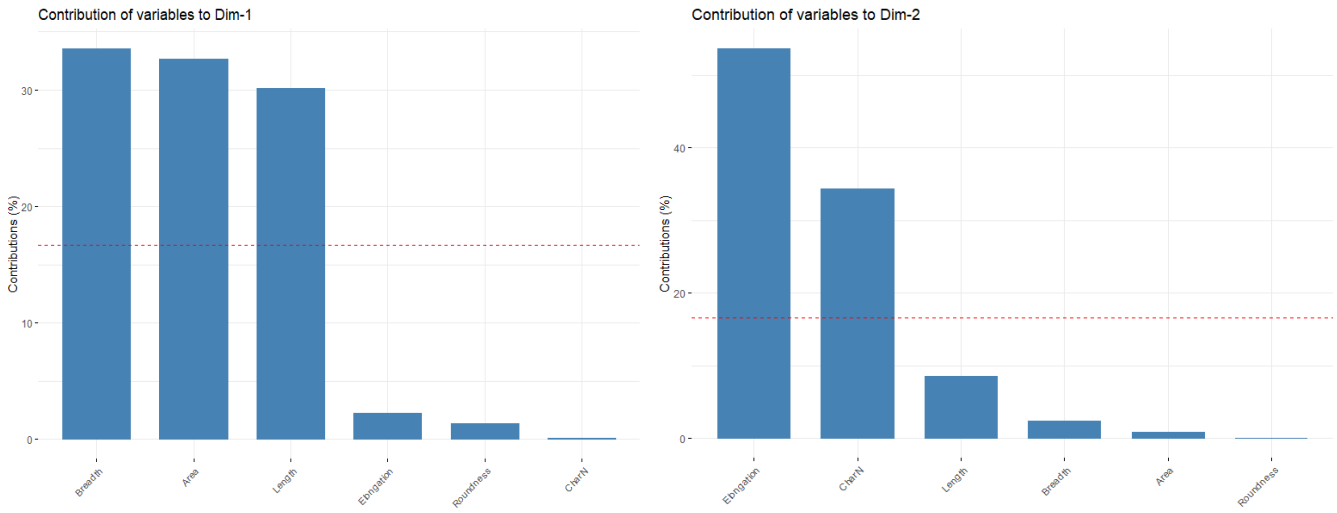

Supplementary Figure 6. The contribution of variables of ocean microcharcoal to principal components

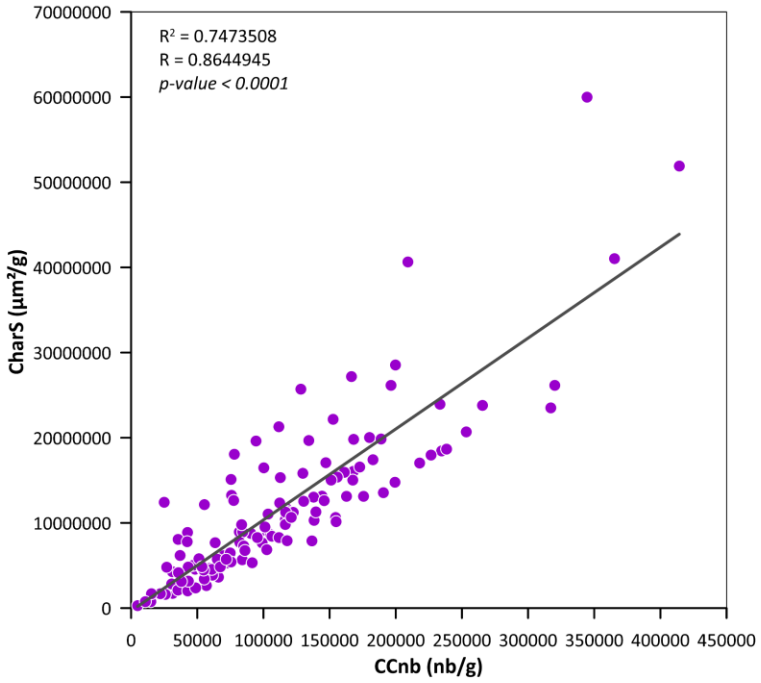

Supplementary Figure 7 Scatter plot of microcharcoal concentration (Ccnb) and surface area (CharS) and associated correlation coefficient

Supplementary Table 2. List of land cover classes (CCI-LC) corresponding to burnt vegetation from FRY database and reclassification into growth habitats (this study)

Label	Value	Category	Growth Habitat	Class
No Data	0			NB
Cropland, rainfed	10	Cropland	GRAMINOIDS	OPEN
Herbaceous cover	11	Herbaceous cover	GRAMINOIDS	OPEN
Tree or shrub cover	12	Tree or shrub cover	GRAMINOIDS	OPEN

Cropland, irrigated or post-flooding	20	Cropland	GRAMINOIDS	OPEN
Mosaic cropland (>50%) / natural vegetation (tree, shrub, herbaceous cover) (<50%)	30		GRAMINOIDS	OPEN
Mosaic natural vegetation (tree, shrub, herbaceous cover) (>50%) / cropland (<50%)	40	Mosaic tree, shrub, herbaceous cover	MIXED	MIXED/OPEN
Tree cover, broadleaved, evergreen, closed to open (>15%)	50	Tree cover, broadleaved, evergreen,	TREE	CLOSED
Tree cover, broadleaved, deciduous, closed to open (>15%)	60	Tree cover, broadleaved, deciduous	TREE	CLOSED
Tree cover, broadleaved, deciduous, closed (>40%)	61		TREE	CLOSED
Tree cover, broadleaved, deciduous, open (15-40%)	62		TREE	CLOSED
Tree cover, needleleaved, evergreen, closed to open (>15%)	70	Tree cover, needleleaved, evergreen	TREE	CLOSED
Tree cover, needleleaved, evergreen, closed (>40%)	71		TREE	CLOSED
Tree cover, needleleaved, evergreen, open (15-40%)	72		TREE	CLOSED
Tree cover, needleleaved, deciduous, closed to open (>15%)	80	Tree cover, needleleaved, deciduous	TREE	CLOSED
Tree cover, needleleaved, deciduous, closed (>40%)	81		TREE	CLOSED
Tree cover, needleleaved, deciduous, open (15-40%)	82		TREE	CLOSED

Tree cover, mixed leaf type (broadleaved and needleleaved)	90	Tree cover, broadleaved and needleleaved	TREE	CLOSED
Mosaic tree and shrub (>50%) / herbaceous cover (<50%)	100	Mosaic tree, shrub, herbaceous cover	MIXED	MIXED/CLOSED
Mosaic herbaceous cover (>50%) / tree and shrub (<50%)	110		MIXED	MIXED/OPEN
Shrubland	120	Shrubland	MIXED	OPEN
Evergreen shrubland	121		MIXED	OPEN
Deciduous shrubland	122		MIXED	OPEN
Grassland	130	Grassland	GRAMINOID	OPEN
Lichens and mosses	140	Lichens and mosses		OPEN
Sparse vegetation (tree, shrub, herbaceous cover) (<15%)	150	Sparse vegetation	GRAMINOID	OPEN
Sparse tree (<15%)	151		GRAMINOID	OPEN
Sparse shrub (<15%)	152		GRAMINOID	OPEN
Sparse herbaceous cover (<15%)	153		GRAMINOID	OPEN
Tree cover, flooded, fresh or brakish water	160	Tree cover, flooded	TREE	CLOSED
Tree cover, flooded, saline water	170		TREE	CLOSED
Shrub or herbaceous cover, flooded, fresh/saline/brackish water	180	Shrub/Herbaceous cover	MIXED	OPEN
Urban areas	190	Other	Other	NB
Bare areas	200			NB
Consolidated bare areas	201			NB
Unconsolidated bare areas	202			NB
Water bodies	210			NB
Permanent snow and ice	220			NB

Supplementary Figure 8 Boxplot of mean elongation ratio for charcoal assemblages in recategorized zones including Western Central Africa (N) with Gulf of Guinea, Congo and Angola where fires spread in tree-dominated vegetation and Southern Africa (S) with Namibia, Orange, Western South Africa, Eastern South Africa and Limpopo where fires spread in graminoid-mixed/shrubs vegetation

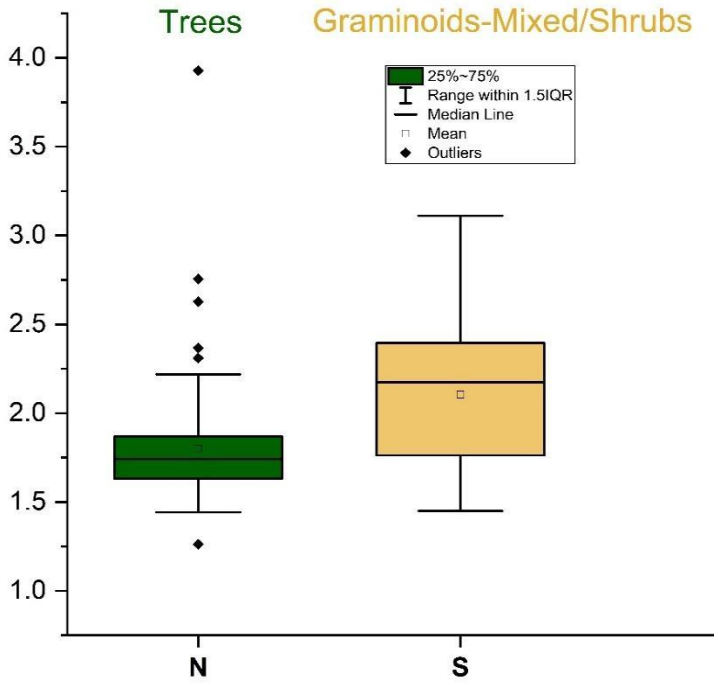

Supplementary References

1. Viegas D.X. 1997. Convective Processes in Forest Fires in Stocks, B.J. and Kauffman, J.B. 1997: Biomass consumption and behavior of Wildland fires in boreal, temperate, and tropical ecosystems
2. Garstang M., Tyson P.D., Cachier H., Radke L. 1997. Atmospheric transports of particulate and gaseous products by fires. In: Clark JS, Cachier H, Goldammer JG, Stocks B (eds). Sediment Records of Biomass Burning and Global Change, 1997; 207-50.
3. Palmer, T.Y, Northcutt, L.I., 1975. Convection columns above large experimental fires, Fire Technology 11(2):111-118.
4. Patterson, W.A., Edwards, K.J., Maguire, D.J., 1987. Microscopic charcoal as a fossil indicator of fire. Quat. Sci. Rev. 6, 3–23. https://doi.org/10.1016/0277-3791(87) 90012-6.

5. Clark, J.S., 1988. Particle motion and the theory of charcoal analysis: source area, transport, deposition, and sampling. Quat. Res. 30, 67–80. https://doi.org/10.1016/ 0033-5894(88)90088-9.
6. Radke, L.R. et al. 1991. Particulate and Trace Gas Emissions from Large Biomass Fires in North America. Proceedings of the Chapman Conference on Global Biomass Burning: Atmospheric, Climate, and Biospheric Implications.
7. Viegas D.X. 1998. Convective Processes in Forest Fires. In: Plate E.J., Fedorovich E.E., Viegas D.X., Wyngaard J.C. (eds) Buoyant Convection in Geophysical Flows. NATO ASI Series (Series C: Mathematical and Physical Sciences), vol 513. Springer, Dordrecht. https://doi.org/10.1007/978-94-011-5058-3_17
8. Peters, M.E., Higuera, P.E., 2007. Quantifying the source area of macroscopic charcoal with a particle dispersal model. Quat. Res. 67, 304e310. https://doi.org/10.1016/j.yqres.2006.10.004.
9. Vachula, R.S., Richter, N., 2017. Informing sedimentary charcoal-based fire reconstructions with a kinematic transport model. The Holocene. https://doi.org/ 10.1177/0959683617715624, 095968361771562.
10. Whitlock, C., Larsen, C., 2002. Charcoal as a Fire Proxy. In: Tracking Environmental Change Using Lake Sediments. Kluwer Academic Publishers, Dordrecht, pp. 75–97. https://doi.org/10.1007/0-306-47668-1_5.
11. Clark, J.S., Lynch, J., Stocks, B.J., Goldammer, J.G., 1998. Relationships between charcoal particles in air and sediments in west-Central Siberia. The Holocene 8, 19–29. https://doi.org/10.1191/095968398672501165.
12. Chrzazvez J. et al., 2014. Impact of post-depositional processes on charcoal fragmentation and archaeobotanical implications: experimental approach combining charcoal analysis and

biomechanics, Journal of Archaeological Science, 44:30-42,https://doi.org/10.1016/j.jas.2014.01.006.

13. Umbanhowar, C.E., McGrath, M.J., 1998. Experimental production and analysis of microscopic charcoal from wood, leaves and grasses. Holocene 8, 341e346.https://doi.org/10.1191/095968398666496051.
14. Mastrolonardo, G. et al., 2017. Size fractionation as a tool for separating charcoal of different fuel source and recalcitrance in the wildfire ash layer. Sci. Total Environ. 595, 461–471.
15. Clark, J.S., Lynch, J., Stocks, B.J., Goldammer, J.G., 1998. Relationships between charcoal particles in air and sediments in west-Central Siberia. The Holocene 8, 19–29. https://doi.org/10.1191/095968398672501165.
16. Zhao, X., Dupont, L.M., Meadows, M.E., Wefer, G. 2016. Pollen distribution in the marine surface sediments of the mudbelt along the west coast of South Africa. Quaternary International, 404. 44-56. doi:10.1016/j.quaint.2015.09.032
17. Patterson, W.A., Edwards, K.J., Maguire, D.J., 1987. Microscopic charcoal as a fossil indicator of fire. Quat. Sci. Rev. 6, 3–23. https://doi.org/10.1016/0277-3791(87) 90012-6.
18. Clark, J.S., 1988. Particle motion and the theory of charcoal analysis: source area, transport, deposition, and sampling. Quat. Res. 30, 67–80. https://doi.org/10.1016/ 0033-5894(88)90088-9.
19. Birks, H. J. B., Birks H., 1980. Quaternary Research. Edward Arnold, London. 289 pp.
20. Stocks, B.J., Kauffman, J.B. 1997. Biomass consumption and behavior of wildland fires in boreal, temperate, and tropical ecosystems: parameters necessary to interpret historic fire regimes and future fire scenarios, pp. 169–188 in J.S. Clark, H. Cachier, J.G. Goldammer, and B.J. Stocks, eds. Sediment Records of Biomass Burning and Global Change. NATO ASI Series, Subseries 1, Global Environmental Change, Vol. 51, Springer-Verlag, Berlin.

21. Clark, J.S., and Royall, P.D. 1996. Local and regional sediment charcoal evidence for fire regimes in presettlement north-eastern North America. J. Ecol. 84: 365-382

22. Lynch, J.A., Clark, J.S., Stocks, B.J. 2004. Charcoal production, dispersal, and deposition from the Fort Providence experimental fire: interpreting fire regimes from charcoal records in boreal forests. Can. J. For. Res. 34, 1642–1656. https://doi.org/10.1139/ x04-071.

23. MacDonald, G. M., Larsen, C. P. S., Szeicz, J. M., Moser, K. A. 1991. The reconstruction of boreal forest fire history from lake sediments: A comparison of charcoal, pollen, sedimentological, and geochemical indices. Quaternary Science Reviews, 10(1), 53–71. https://doi.org/10.1016/0277-3791(91)90030-X

24. Tinner, W. et al. 1998. Pollen and charcoal in lake sediments compared with historically documented forest fires in southern Switzerland since ad 1920. Holocene, **8**, 31–42.

25. Nichols, G.J. et al. 2000. Experiments in waterlogging and sedimentology of charcoal: results and implications. Palaeogeography, Palaeoclimatology, Palaeoecology **164**: 43–56.

26. Hooghiemstra H. et al. 2006. Late Quaternary palynology in marine sediments: A synthesis of the understanding of pollen distribution patterns in the NW African setting, Quaternary International, 148:1, 29-44, https://doi.org/10.1016/j.quaint.2005.11.005.

27. Dupont, LM; Marret, Fabienne M.; Kyaw W. 1998. Land-sea correlation by means of terrestrial and marine palynomorphs from the equatorial East Atlantic: phasing of SE trade winds and the oceanic productivity. Palaeogeography, Palaeoclimatology, Palaeoecology, 142(1-2), 51-84, https://doi.org/10.1016/S0031-0182(97)00146-6

28. Dupont, L.M., Linder, H.P., Rommerskirchen, F. Schefuß, E. 2011. Climate-driven rampant speciation of the cape flora. Journal of Biogeography, 38(6). 1059-1068. doi:10.1111/j.1365-2699.2011.02476.x

29. Draxler, R. R., G. D. Hess, 1998. An overview of the HYSPLIT_4 modelling system for trajectories, dispersion, and deposition. Aust. Meteor. Mag., 47, 295–308.
30. Sofiev, M., Siljamo, P., Ranta, H., Linkosalo, T., Jaeger, S., Rasmussen, A., Rantio- Lehtimaki, A., Severova, E., Kukkonen, J., 2013. A numerical model of birch pollen emission and dispersion in the atmosphere. Description of the emission module. Int. J. Biometeorol. 57, 45-58. https://doi.org/10.1007/s00484-012-0532-z
31. Vachula, R.S., Richter, N., 2017. Informing sedimentary charcoal-based fire reconstructions with a kinematic transport model. The Holocene. https://doi.org/ 10.1177/0959683617715624095968361771562.
32. Dare, R.A., 2015. Sedimentation of volcanic ash in the HYSPLIT dispersion model. CAWCR Technical Report No. 079. Melbourne: Centre for Australian Weather and Climate Research.
33. Vachula, R.S., Russell, J.M., Huang, Y., Richter, N., 2018. Assessing the spatial fidelity of sedimentary charcoal size fractions as fire history proxies with a high-resolution sediment record and historical data. Palaeogeogr. Palaeoclimatol. Palaeoecol. 508, 166–175. https://doi.org/10.1016/j.palaeo.2018.07.032.
34. Peters, M.E., Higuera, P.E., 2007. Quantifying the source area of macroscopic charcoal with a particle dispersal model. Quaternary Research 67, 304–310.
35. Vachula, R. S., Richter, N. 2018. Informing sedimentary charcoal-based fire reconstructions with a kinematic transport model. The Holocene, 28(1), 173–178. https://doi.org/10.1177/0959683617715624
36. Hubert Bernard (2014). Atelier de Réflexion Prospective (ARP) MERMED : Adaptation aux changements environnementaux en mer Méditerranée : quelles recherches et quels partenariats ?

Synthèse des fiches prospectives: Le bassin méditerranéen à l'horizon 2030 : Quels défis à relever pour la mer Méditerranée ? https://archimer.ifremer.fr/doc/00375/48660/

37. de Baar, Hein J W; et al. (1989): JGOFS North Atlantic R.V. Tyro Leg 2 of the cruise in 1989, Upper Ocean Processes. Unpublished Cruise report, Royal Netherlands Institute for Sea Research, Texel, The Netherlands
38. Hall Ir, Hemming Sr, Levay Lj, Expedition 361 Scientists (2016). Expedition 361 Preliminary Report: South African Climates (Agulhas LGM Density Profile) 30 January–31 March 2016. International Ocean Discovery Program. https://doi.org/10.14379/iodp.pr.361.2016
39. Cochonat, P., 1998. ZAIANGO2 cruise, RV L'Atalante, http://dx.doi.org/10.17600/98010110
40. Savoye, B., 1998. ZAIANGO1 cruise, RV L'Atalante, http://dx.doi.org/10.17600/98010100
41. Savoye, B., Ondréas, H., 2000. ZAIANGOROV cruise, RV L'Atalante.
42. Schefuß, E., G. J. M. Versteegh, J. H. F. Jansen and J. S. Sinninghe Damsté (2004). "Lipid biomarkers as major source and preservation indicators in SE Atlantic surface sediments." Deep-Sea Research, Part I 51: 1199-1228
43. Osmont, D. et al. 2020. Tracing devastating fires in Portugal to a snow archive in the Swiss Alps: a case study, The Cryosphere, 14, 3731–3745, https://doi.org/10.5194/tc-14-3731-2020.
44. Dietze, E. et al. 2020. Relationships between low-temperature fires, climate and vegetation during three late glacials and interglacials of the last 430 kyr in northeastern Siberia reconstructed from monosaccharide anhydrides in Lake El'gygytgyn sediments, Clim. Past, 16, 799–818, https://doi.org/10.5194/cp-16-799-2020.
45. Legrand, M. et al., 2016. Boreal fire records in Northern Hemisphere ice cores: a review, Clim. Past, 12, 2033–2059, https://doi.org/10.5194/cp-12-2033-2016

46. Grieman, M. M., Aydin, M., Isaksson, E., Schwikowski, M., Saltzman, E. S. 2018. Aromatic acids in an Arctic ice core from Svalbard: a proxy record of biomass burning, Clim. Past, 14, 637–651, https://doi.org/10.5194/cp-14-637-2018

47. Hicks, S., and Isaksson, E. 2006. Assessing source areas of pollutants from studies of fly ash, charcoal, and pollen from Svalbard snow and ice, J. Geophys. Res., 111, D02113, doi:10.1029/2005JD006167.

48. Snitker, G., 2018. Identifying natural and anthropogenic drivers of prehistoric fire regimes through simulated charcoal records. J. Archaeol. Sci. 95, 1–15.

49. Davis, R.B. 1967. Pollen studies of near-surface sediments in Maine lakes. In Cushing E.J. and Wright HE (eds), Qauternary Paleoecology, pp. 1430173. Yale University Press, New Haven

50. Dupont, L., Wyputta, U., 2003. Reconstructing pathways of aeolian pollen transport to the marine sediments along the coastline of SW Africa. Quat. Sci. Rev. 22,157-174. https://doi.org/10.1016/S0277-3791(02)00032-X.

51. Dupont, LM, Caley, T and Castañeda, IS. 2019. Effects of atmospheric CO2 variability of the past 800 kyr on the biomes of southeast Africa. Climate of the Past, 15(3). 1083-1097. doi:10.5194/cp-15-1083-2019

52. Hooghiemstra, H et al. 1986. Pollen and spore distribution in recent marine sediments: a record of NW-African seasonal wind patterns and vegetation belts. Meteor Forschungsergebnisse, Deutsche Forschungsgemeinschaft, Reihe C Geologie und Geophysik, Gebrüder Bornträger, Berlin, Stuttgart, C40, 87-135

53. Zhao, X, Dupont, LM, Meadows, ME and Wefer, G. 2016. Pollen distribution in the marine surface sediments of the mudbelt along the west coast of South Africa. Quaternary International, 404. 44-56. doi:10.1016/j.quaint.2015.09.032